NJC

Accepted Manuscript

This is an *Accepted Manuscript*, which has been through the Royal Society of Chemistry peer review process and has been accepted for publication.

Accepted Manuscripts are published online shortly after acceptance, before technical editing, formatting and proof reading. Using this free service, authors can make their results available to the community, in citable form, before we publish the edited article. We will replace this *Accepted Manuscript* with the edited and formatted *Advance Article* as soon as it is available.

You can find more information about *Accepted Manuscripts* in the Information for Authors.

Please note that technical editing may introduce minor changes to the text and/or graphics, which may alter content. The journal's standard Terms & Conditions and the Ethical guidelines still apply. In no event shall the Royal Society of Chemistry be held responsible for any errors or omissions in this *Accepted Manuscript* or any consequences arising from the use of any information it contains.

ROYAL SOCIETY OF CHEMISTRY

www.rsc.org/njc

Cite this: DOI: 10.1039/c0xx00000x

www.rsc.org/xxxxxx

ARTICLE TYPE

Enhanced hydrogen production under visible light source and dye degradation under natural sunlight using nanostructured doped zinc orthotitanates

Latesh Nikam[a,b], Rajendra Panmand[a], Sunil Kadam[a], Sonali Naik[a] and Bharat Kale[a]*

Received (in XXX, XXX) XthXXXXXXXXX 20XX, Accepted Xth XXXXXXXXX 20XX
DOI: 10.1039/b000000x

The nanostructured Ag and Co doped zinc orthotitanate (ZOT) were synthesized using combustion method. The structural and optical analysis shows the existence of cubic and tetragonal phases. Morphological study by FESEM reveals the formation of web like structure along with pot holes by self-assembling of spherical nanoparticles of ~ 50 nm size. Further, TEM investigations reveal diffused and uneven shaped nanoparticles in the range of 10-25 nm. BET surface area measurements show decrease in surface area due to doping. These ZOT's were employed for photocatalytic dye degradation (Acid Orange -8 and Rhodamine –B) under natural sunlight. The prima facie observations showed Ag@ Zn_2TiO_4 to be an excellent photocatalyst for dye degradation. Kinetic study shows the order of the reaction in the range 1.1-1.41. The ZOT's synthesized have been also used for the photocatalytic hydrogen production from H_2S under visible light irradiation. It is noteworthy that utmost H_2 production (2784 µmol/h/100 mg) was observed for Ag@Zn_2TiO_4 which is much higher amongst the visible light active photocatalyst reported so far. The dye degradation and hydrogen production from H_2S using ZOT is hitherto unattempted. The nanostructured Zn_2TiO_4 will be a potential visible light active photocatalyst for waste degradation and water splitting.

1 Introduction

Zn_2TiO_4 alias zinc orthotitanate (ZOT) is the stable phase of ZnO-TiO_2 system which has been employed for various applications like microwave dielectrics, catalyst, photocatalyst, pigment, gas sensing material, antistatic films and anti-reflecting coating in solar cells.[1,2] ZnO-TiO_2 system can generate five compounds namely zinc orthotitanate (Zn_2TiO_4), zinc metatitanate ($ZnTiO_3$), $Zn_2Ti_2O_6$, $Zn_2Ti_3O_8$ and $Zn_4Ti_5O_{16}$ [3], but only $ZnTiO_3$, Zn_2TiO_4 and $Zn_2Ti_3O_8$ are found to be stable.[4-6] Phase formation temperature of zinc titanates varies with preparation method and Zn/Ti ratio of the precursors.[7-10] Zn_2TiO_4 have been synthesized from ZnO and TiO_2 by solid state reaction route at high temperature (1200 °C).[11]The nanostructured Zn_2TiO_4 has also been synthesized by flame spray pyrolysis [12]and sol-gel method.[13] Very limited literature is available on metal doped Zn_2TiO_4. Cu doped Zn_2TiO_4 has been reported with enhanced microwave dielectric properties as compared to Zn_2TiO_4.[14] Ceramic pigments of the spinel structure were obtained by synthesizing Co, Ni, and Mn doped Zn_2TiO_4 using polymeric precursor method.[15] The Cr^{+3}, V^{+5} and Sn^{+4} doped nanostructured Zn_2TiO_4 have also synthesized by polymeric precursor method and their optical properties have been studied in detail.[1]

Being an efficient gas adsorbent, Zn_2TiO_4 has been effectively used for removal of multiple constituents of hot stream gases.[16] The regeneration of Zn_2TiO_4 was found to be faster with negligible loss. Its thermal stability is higher than the parent metal oxides.[17] *Shiqiang Hao et.al*. have theoretically interpreted surface reaction of H_2S on 010 surface of Zn_2TiO_4. On the basis of DFT calculations, it has been concluded that 010 surface is having a large fraction of the total surface area of Zn_2TiO_4 and having two distinct terminations, i.e. one oxygen rich and other metal rich.[18] H_2S can be adsorbed effectively at Zn sites leading to its dissociation, due to low adsorption energy (-0.75 eV). These theoretical findings suggest that Zn_2TiO_4 can be used as visible light photo catalyst for dissociation of H_2S to generate H_2, if band gap tuned to the visible region. Zn_2TiO_4 being good adsorbent for H_2S and having band gap around 3.1 eV could be candidate for photocatalytic decomposition of H_2S. These findings lead us to attempt H_2S splitting using zinc orthotitanates.

H_2S is harmful to human health as well as environment being pollutant in water and air. Techniques like adsorption of H_2S on Zn_2TiO_4, Claus process, photocatalytic degradation etc. have been employed for removal of H_2S from water. Various researchers have attempted to remove H_2S from aqueous solution by photocatalytic degradation using sulphides as photocatalyst which generates clean and eco-friendly hydrogen fuel.[19-26] Use of

metal oxides for the same purpose has been less explored.

Ubiquitously, dyes are well known for their toxic and hazardous nature to mankind. Azo dyes produce toxic aromatic amine and have harmful environmental effects. Since, they have very low degradation rate by aerobic treatment process, many dye molecules are resistant to biological degradation.[27]

Acid Orange -8(AO-8) is water soluble dye containing mono azo group and has been widely used for dying silk fibre. It is toxic and carcinogenic in nature, hence it is essential to take systematic steps for the removal or degradation of AO-8. *Preeti Mehta et. al*. studied photocatalytic degradation of AO-8 using TiO_2 under visible light irradiation at various pH and concentration of AO-8. [28]

Rhodamine B (Rh-B) is a xanthene dye widely used as colorant in textile and water tracer fluorescent. Rh-B is harmful if swallowed by human being and animals which causes irritation to skin, eyes and respiratory track. The carcinogenicity, reproductive and developmental toxicity, neurotoxicity and chronic toxicity towards human and animals is well known.[29]

Photocatalytic degradation of AO-8 is rarely studied and it has been observed that photocatalytic activity of ZnO towards degradation of AO-8 is less than TiO_2 under visible light irradiation.[30] Researchers have attempted photocatalytic degradation of Rhodamine-B by using doped and undoped ZnO and TiO_2 [31-33] and other photocatalysts.[34,35] However, very limited study has been reported on photocatalytic degradation by Zn_2TiO_4.[36-38] The photocatalytic H_2 generation from water-methanol solution was attempted by using $Zn_2Ti_{1-x}Fe_xO_4$ under visible light.[39a]

Considering the stability of the spinel Zn_2TiO_4, there is wide scope for doped Zn_2TiO_4 as a visible light active photocatalyst for dye degradation and more significantly for H_2 production. In view of this, we have explored the study on Zn_2TiO_4 and its use as visible light photocatalyst for photo degradation of dyes as well as photo hydrogen production from H_2S.

In the present investigation, we have demonstrated the synthesis of nanostructured spinel $Zn_2TiO_4$by combustion method. The authors already reported synthesis of Zn_2TiO_4 and $Ag@Zn_2TiO_4$[39b]. We are reporting herewith synthesis of $Co@Zn_2TiO_4$ by combustion method for the first time. More significantly, these zinc orthotitanates are employed as visible light photocatalyst for Acid orange (AO-8), Rhodamine–B (Rh-B) degradation and H_2S splitting to produce H_2 which is hitherto unattempted.

2 Experimental Section

2.1 Synthesis of zinc orthotitanates by combustion method

Zinc acetate, titanium tetraisopropoxide (TTISP), citric acid, ammonium nitrate were taken in 1:0.5: 5:5 mole proportions along with 2.5 g starch. The homogeneous paste was prepared in isopropanol and methanol. Paste was kept overnight to obtain uniform mixture. Paste was dropped stepwise into preheated tubular furnace at 650 °C and 750 °C and heating continued for 3 h after completion of dropping. For synthesis of Ag and Co doped zinc orthotitanates, silver nitrate and cobalt acetate were taken in stoichiometric proportion for synthesis of$Zn_{1.9}Ag_{0.1}TiO_4$and $Zn_{1.9}Co_{0.1}TiO_4$,respectively.[39b] The zinc orthotitanates synthesized are further characterized using sophisticated techniques.

2.2 Characterization

The UV-vis absorption spectra of the as synthesized metal oxides were recorded on Perkin Elmer UV-Vis spectrophotometer in the 300-900 nm range using pure $BaSO_4$ as reference. Photo Luminance spectra were recorded on PL-Shimadzu instrument (RF-5301 PC) at room temperature in aqueous dispersion state at excitation wavelength 300 nm. XRD patterns were recorded in ambient air at room temperature on D-8 Advanced X-ray diffractometer using Cu -Kα radiation (λ= 0.15418 nm) at the scan rate of 0.1° /min in the 2θ range 10-90°. FTIR spectra were recorded on Perkin Elemer IR spectrophotometer in the range 350-4000 cm^{-1}. Field Emission Scanning Electron Microscopy (FESEM) images were obtained on HITACHI 4800 instrument. For obtaining FESEM images, the powder sample dispersed in methanol by sonication was loaded on Al foil. Transmission Electron Microscopy (TEM) micrographs were obtained by using Philips (CM-200) instrument at 80 KV. For TEM images, powder sample dispersed in ethanol by sonication and loaded on copper grid coated with holey carbon support film. Surface area was measured by the Brunauer Emmett Teller (BET) method (make/model-Micromeritics, ASAP 2010) from Nitrogen adsorption-desorption isotherm at 77 K. . Pore diameter and pore volume was determined by Barrete-Joyner-Halenda (BJH) method. Elemental analyses of the compounds were performed by EDXRF (ARL QUANT'X , Thermofischer) analyses .

2.3 Photocatalytic dye degradation

Photocatalytic dye degradation was studied under the sunlight using photocatalytic reactor designed in our laboratory. The desired quantity of the photocatalyst was added in 40 ml aqueous solution of the dye (AO-8 and Rh-B). The mixture was sonicated for 10 min and magnetically stirred for 20 min in dark to establish adsorption-desorption equilibrium. The suspension was irradiated under sun light during 11.00 am to 3.00 pm in the month of March and April. Intensity of sunlight was recorded using Lux meter (Lutron, LX-107HA) . Concentration of dye in the aqueous solution was measured by sampling small quantity of suspension at specific time interval. The solid catalyst was separated by centrifugation at 5000 rpm for 10 min. The concentration of dye was determined from absorbance at λ_{max} of the AO-8 (492 nm) and Rh-B (552 nm) using UV-Vis spectrophotometer.

2.4 Photocatalytic H_2S splitting for H_2 generation

H_2S splitting was carried out on photocatalytic system developed in our laboratory under visible light source 300 W (Lot Orel group, Europa, LSH302). The in-house designed photocatalytic system consist of H_2S gas generator, bubble trap , water jacketed photocatalytic reactor, H_2S gas trap and graduated H_2 gas measuring cylinder . The photocatalyst (100 mg) was uniformly

mixed in 175 ml 0.25 N KOH by magnetic stirring followed by purging with Ar gas for about 15 min. Reactor was maintained at room temperature by continuous water circulation through water jacket surrounding the reactor. H_2S gas prepared using microscale gas generator was bubbled into the suspension at the rate 2.0 $ml.min^{-1}$ for about 90 min for the purpose of saturation. Irradiation of the reactor started after the saturation of the suspension with H_2S. Gas generated was allowed to pass through H_2S traps charged with 50 ml 0.5 N NaOH to ensure the collection of pure H_2 gas. The H_2S flow at 2.0 $ml.min^{-1}$ was maintained constant throughout the process carried out for 3 h. Volume of the gas generated was measured at suitable time interval. H_2 gas was immediately transferred into rubber bladder. H_2 gas evolved was confirmed by GC analyses (Model: Shimadzu (GC-14B), MS- 5 °A Column , TCD, Ar carrier).

3 Results and Discussion

3.1 Synthesis

Zn_2TiO_4 has been synthesized by combustion method using titanium tetraisopropoxide (TTISP) , zinc acetate precursors and citric acid , starch as fuel and ammonium nitrate as an oxidizer. We have used complex fuel system because it favours formation of nanosized particles.[40] When ammonium nitrate decomposes, it releases oxygen which can be used by fuel i.e. citric acid and starch. Citric acid forms complex with Zinc (II) and Ti (IV) which facilitates homogeneous mixture in the gel as well as it is the source of C and H which produce CO_2 and H_2O accompanied by liberation of heat.[41]Hence, due to high exothermicity, the phase formation is obtained at low temperature as compared to solid state reaction (>1000°C).[39,42-44] Mixture of ZnO and TiO_2 has been formed when the combustion was performed at 550-600 °C. After several trials at various temperatures, desired phase has been formed at 650 °C. It is quite understood that due to liberation of huge amount of gases during thermal shock at 650 °C, the nanocrystalline product is formed. [45]

In combustion technique employed, the chelating agents like citric acid forms complex with the metal cations which upon thermal decomposition forms carbonaceous matrix which act as a substrate for homogeneous distribution of metal oxide phase. Extensive distribution of mesoporous carbonaceous matrix provides large number of well separated nucleation sites for formation of oxide. This helps in obtaining particles with lower size distribution. Following combustion reaction takes place during the combustion at 650 °C. [46]

$$2Zn(CH_3COOH)_2.2H_2O + Ti(CH_3CH_2COO)_4 + 10NH_4NO_3 + 10C_6H_8O_7 + x(C_6H_{10}O_5)_n + [59+6nx]O_2 \rightarrow Zn_2TiO_4 + [80+6nx]CO_2 + [82+5nx]H_2O + 10N_2 \quad (1)$$

Where 'n' is number of monomers in starch and 'x' is number of moles corresponding to amount of starch taken. The zinc orthotitanates obtained at 650 °C were further characterized for structural, morphological and photocatalytic studies.

3.2 Structural study:

3.2.1 XRD analyses

Fig. 1 represents XRD pattern of the metal oxide synthesized, which contains peaks due to Zn_2TiO_4 and ZnO. The XRD pattern shows the existence of spinel structure of Zn_2TiO_4. Peaks due to Zn_2TiO_4 are in good agreement with tetragonal phase [JCPDS card No. 86-0158 (ESI -S1)] , a= 6.006 A°, b=8.415 A°] [47] as well as cubic phase.[JCPDS Card No. 86-0154 (ESI, S1), a=8.469 A°] .[48] The presence of two phases has been discussed thoroughly by Robert Millard et. al.[42] According to their findings, tetragonal phase along with cubic phase exists in the temperature range 490-555 °C and extent of cubic phase increases with increase in temperature. Hence, cubic phase can be formed at higher temperature and mixed phases at lower temperature which is quite justifiable. However, it is quite difficult to obtain single phase in case of zinc orthotitanate at lower temperature.[49] The further evidences have been discussed in optical properties.

Comparative XRD of Zn_2TiO_4 and Ag@ Zn_2TiO_4 is shown in the Figure 2. XRD pattern of Ag@ Zn_2TiO_4 depicts additional peaks due to Ag [JCPDS card No. 04-0783 (ESI, S1), cubic, a=4.086 A°] element along with the peaks of Zn_2TiO_4 and ZnO [JCPDS card No. 89-1397, hexagonal, a=3.253 A°, c=5.213 A°] indicate nancomposite formation of Ag-ZnO- Zn_2TiO_4.[50,51] It means, AgO is not formed during the combustion, instead elemental Ag has been formed by reduction of Ag^+ during combustion. This may be because of citric acid used during combustion which generally creates reductive atmosphere.[52,53] It is quite well known that silver oxide decompose to silver at high temperature.[54]The isolated sharp peaks due to Ag in XRD indicate presence of Ag on surface of the Zn_2TiO_4.

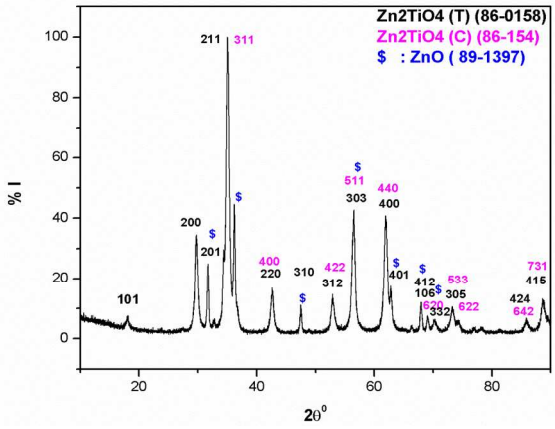

Fig.1: XRD pattern of zinc orthotitanate(Zn_2TiO_4)

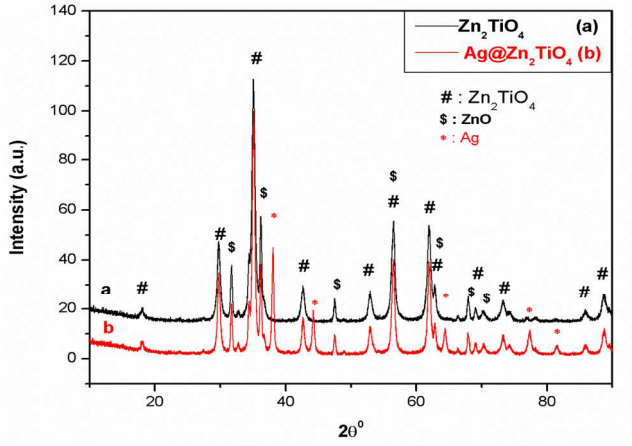

Fig.2 Comparative XRD pattern of a) Zn_2TiO_4 and b)$Ag@Zn_2TiO_4$

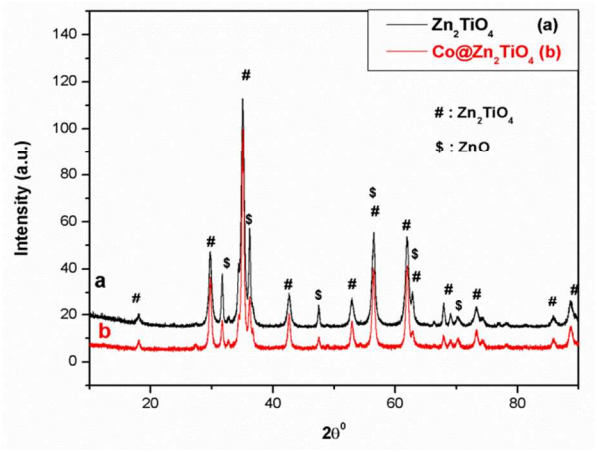

Fig. 3 Comparative XRD pattern of a)Zn_2TiO_4 and b) $Co@Zn_2TiO_4$

Fig. 3 depicts the XRD pattern of Zn_2TiO_4 and $Co@Zn_2TiO_4$. XRD of $Co@Zn_2TiO_4$ (Figure 3b) indicates no additional peaks due to cobalt oxide. It means that Co^{+2} ions have replaced Zn^{+2} ions in the Zn_2TiO_4 lattice and no shifting in 2θ of any peaks is observed. This is because of equivalent ionic size of Zn^{+2} (74 pm) and Co^{+2} (74.5 pm) ions.[55] Thus, as synthesized $Co@Zn_2TiO_4$ will have molecular formula $Zn_{2-x}Co_xTiO_4$ and value of 'x' has been observed to be 0.1 from EDXRF analysis and concentration of precursors, giving the molecular formula $Zn_{1.9}Co_{0.1}TiO_4$. The XRD pattern shows the existence of spinel structure of Zn_2TiO_4 in the case of $Co@Zn_2TiO_4$. *Soraia C Souza et. al.* synthesized Co doped Zn_2TiO_4 by polymeric precursor method and reported that single phase $Zn_{2-x}Co_xTiO_4$ can be formed up to x=0.4.[15]*Hee Kwon Jun et al*. observed that Co replaces one of the zinc atom in Zn_2TiO_4 followed by $ZnCoTiO_4$ formation. General phenomena of the metals are that metal ions having same oxidation number and nearly the same ionic radius which do not affect on XRD pattern. Hence, it is impossible to distinguish between the spinel structure of Zn_2TiO_4 and $ZnCoTiO_4$ by XRD analysis.[56] The average crystallite size was determined using Scherrer equation and observed to be 13 nm for Zn_2TiO_4while, 19 and 18 nm for Zn_2TiO_4 in $Ag@Zn_2TiO_4$ and $Co@Zn_2TiO_4$ respectively. The crystallite size of Ag in $Ag@Zn_2TiO_4$ has been observed to be 21 nm. It was observed that doping leads to an increase in short-range disorder and increase in crystallite size.[1]

3.2.2 FTIR analysis

FTIR spectra of the zinc orthotitanates was taken in the region 4000-350 cm^{-1}(ESI, S2).Bands in the spectral region 1200-4000 cm^{-1} are due to vibration frequencies due to traces of organic residue and adsorbed water.[2]The bands have been observed at ~ 3470 and ~ 1630 cm^{-1} in FTIR spectra of Zn_2TiO_4, $Ag@Zn_2TiO_4$ and $Co@Zn_2TiO_4$. These bands are due to weak physical adsorption of water molecules being originated from stretching and bending vibrations. In this case, existence of the hydroxyl groups is detected even at higher temperature. *T. Ivanova et al.* also observed presence of hydroxyl group at 600 °C in case of thin film of Zn_2TiO_4 system.[2] Bands in the range 1200-4000 cm^{-1} show trace of carbon content even at 650 °C. For complete removal of carbon content, sintering at 1000°C is required. However, at 1000°C particle size will increase leading to formation of macro particles.[57] Broad band at ~ 710 and weak band at ~ 586 cm^{-1} are due to stretching vibration in TiO_6 group present in the Zn_2TiO_4.[2] These peaks are clearly seen in the FTIR spectra as shown in the figure (ESI, S2). Band around 420 cm^{-1} may be due to ZnO_n polyhedron which appears in all zinc titanates.[58] Presence of absorption bands at 575 (b), 475(w), 420(w) and 400 (w) indicates tetragonal phase of Zn_2TiO_4.[59] M-O (M= Ag and Co(II)) bands are not observed may be because of very less % of dopant metal in Zn_2TiO_4. Bands due to anatase and amorphous TiO_2 are also not observed in IR spectra of all synthesized metal oxides. It is very difficult to confirm the absence of TiO_2 and ZnO on the basis of IR frequencies appeared in the range 1000-350 cm^{-1} because, bands due to Zn_2TiO_4, $ZnTiO_3$, ZnO and TiO_2 appears in the same region with minor variation.

3.3 Elemental analyses

The elemental analysis of the synthesized compounds has been performed by Energy Dispersive X ray Fluorescence (EDXRF) analyses technique. The EDXRF analyses (ESI, S3) shows that % Zn , Ti, Ag and Co observed in synthesized samples is in good agreement with expected values and molecular formula of the oxides.

3.4 Morphological study

Morphological study was performed by FESEM (Field Emission Scanning Electron Microscopy) and TEM (Transmission Electron Microscopy) analyses.

FESEM images of Zn_2TiO_4 given in the Fig. 4 shows formation of web like morphology consisting of pot holes. Spherical nanoparticles of the size around 50 nm are self-aligned to form web like morphology. The web like morphology with pot holes may be formed due to evolution of gases during synthesis of Zn_2TiO_4 by combustion method. The evolution of gases favours formation of web like morphology.[41]

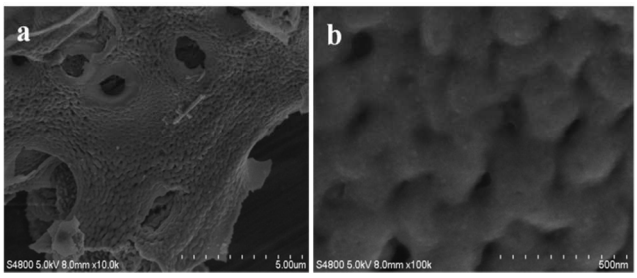

Fig. 4 FESEM images of Zn_2TiO_4 magnified at a) 10 K b) 100 K magnification.

In case of $Ag@Zn_2TiO_4$ (Fig. 5) stacking of layers has been observed with larger pot holes. Despite of increase in pot holes, increase in crystallite size and staking of layers causes lowering in surface area with respect to Zn_2TiO_4.

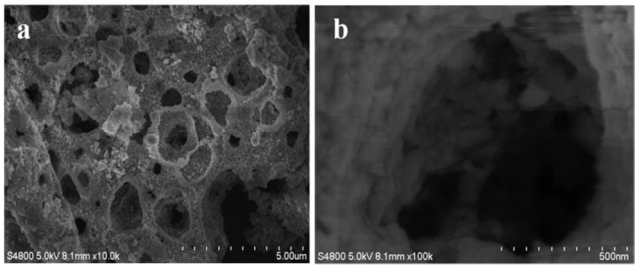

Fig. 5 FESEM micrographs of $Ag@Zn_2TiO_4$ at a) 10 K b) 100 K magnification.

Fig. 6 shows formation of large and thick clusters due to agglomeration of nanoparticles in the case of $Co@Zn_2TiO_4$. Very few pot holes are observed on the cluster (Fig. 6a) as compared to that of in Zn_2TiO_4 and $Ag@Zn_2TiO_4$. Agglomerated spherical particles of the size around 50 nm are clearly seen in the Fig. 6b. Crystallite size also found to be increased with respect to Zn_2TiO_4.

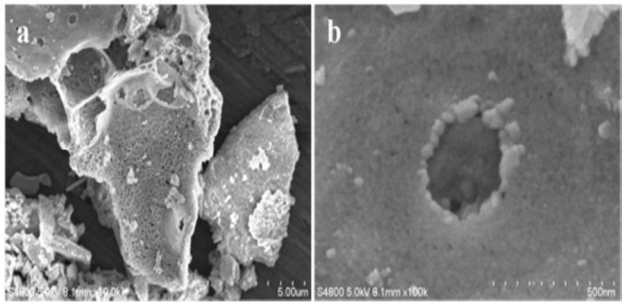

Fig. 6 FESEM micrographs of $Co@Zn_2TiO_4$ at a) 10 K and b) 100 K magnification

In nutshell, lower surface area may be due to agglomeration of nanoparticles in the form of cluster. The doping of Ag and Co disturbs the morphology of doped Zn_2TiO_4 as well as lowers the surface area when synthesized by combustion method.[56,60,61]

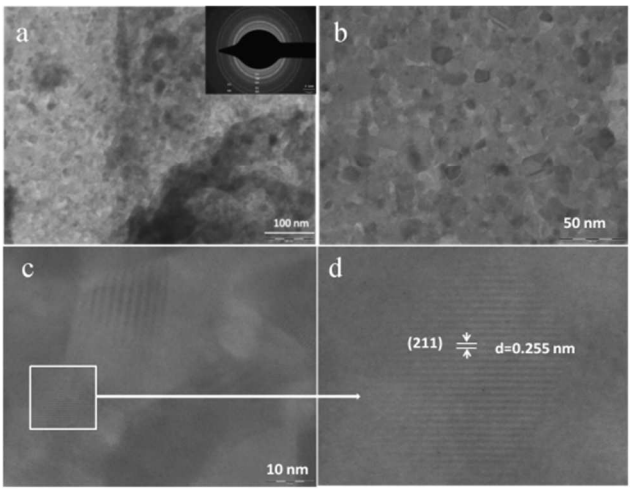

Fig. 7 TEM images of Zn_2TiO_4 a) 100 nm scale and inset ED pattern b) 50 nm scale c) 10 nm scale d) magnified portion of Figure c showing lattice fringes with d211=0.250 nm

TEM images of Zn_2TiO_4 are shown in Fig. 7. Diffused particles of irregular shape having size in the range of 10 nm are observed (Fig. 7b) however, their shape and size is difficult to identify. Lattice fringes corresponding to 211 plane (d_{211}=0.250 nm) are observed (Fig. 7c and d). Uniform and continuous ring pattern observed in ED pattern (inset of Fig. 7a) is due to randomly oriented nanocrystals. The d spacing determined from ED pattern are in good agreement with XRD results.

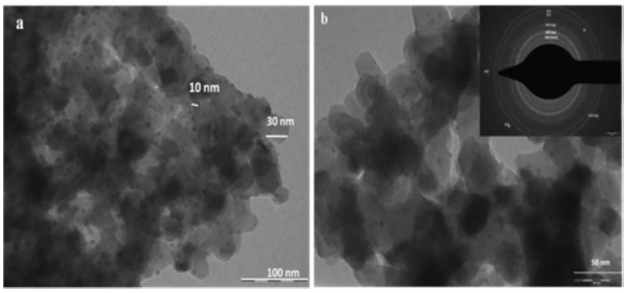

Fig.8 TEM images of $Ag@Zn_2TiO_4$ a) 100 nm scale b) 50 nm scale and inset ED pattern

TEM images of $Ag@Zn_2TiO_4$(Fig. 8) display nanoparticles having size in the range 30-50 nm. Small particles in the range 5-10 nm are found to be embedded into the large particles (Fig. 8a and b), which could be of silver as detected by XRD. ED pattern shows ring pattern (ESI S4) consisting of very fine spots indicating polycrystalline nature and random alignment of nanocrystals of $Ag@Zn_2TiO_4$. The d spacing values obtained from ED pattern (inset of Fig. 8b) reveals the presence of 002 plane of ZnO and 100,220 and 200 planes of Ag along with planes of Zn_2TiO_4. These observations are in agreement with XRD pattern of $Ag@Zn_2TiO_4$.

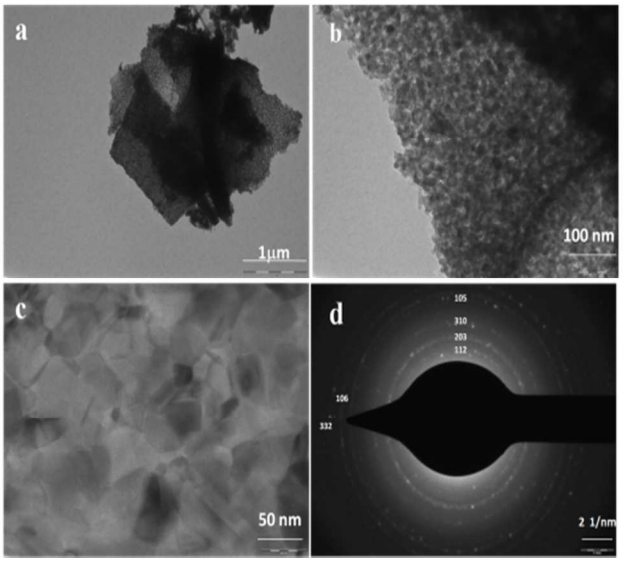

Fig. 9 TEM images of $Co@Zn_2TiO_4$ at, a) 1 µm b) 100 nm c) 50 nm scale and d) ED pattern

TEM images (Fig. 9a & b) of $Co@Zn_2TiO_4$ show alignment of nanoparticles of the size ~ 25 nm lead to form 2-D sheet. High magnification image shows (Fig. 9c) nanoparticles of the size in the range 25-50 nm with uneven shapes (tetragonal and pentagonal). The ED pattern (Fig. 9d) shows bright spotted ring pattern indicating polycrystalline nature of the sample. The d spacing calculated from ED and XRD pattern are in agreement with each other. ED pattern doesn't show rings due to any phase of cobalt oxide which supports interpretation led by XRD pattern of $Co@Zn_2TiO_4$. The intense spotted ring pattern observed for $Ag@Zn_2TiO_4$ and $Co@Zn_2TiO_4$ as compared to that of Zn_2TiO_4shows high degree of crystallinity. It is observed that doping leads to increase in crystal size which ultimately increases the crystallinity. Hence, the increase in polycrystalline nature of the doped Zn_2TiO_4 is quite justifiable.

3.5 Surface study

The surface area of the zinc orthotitanates can be determined from the nitrogen-adsorption isotherms and pore size distribution. The shapes of hysteresis loop of all zinc orthotitanates are of H3 type (Fig. 10). The H3 type of hysteresis loop is associated with mesopores present in the crystal.[62] The pore size distribution (ESI, S5) obtained from the isotherm shows broad pore size distribution for Zn_2TiO_4, $Ag@Zn_2TiO_4$ and $Co@Zn_2TiO_4$, respectively.

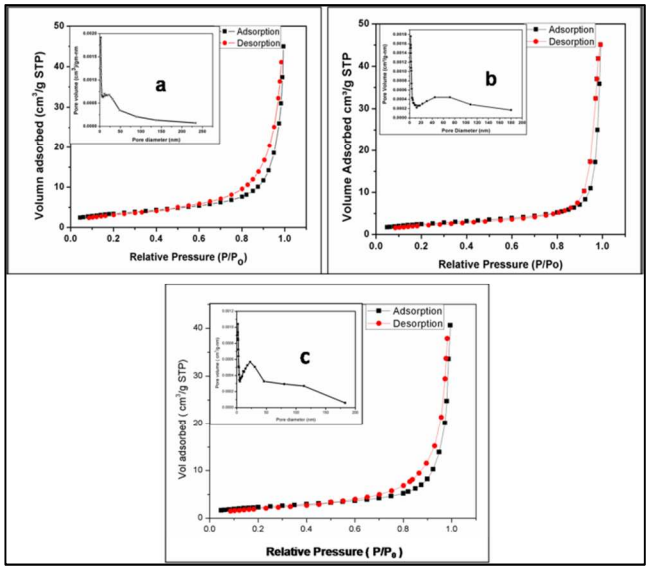

Fig.10 BET adsorption isotherms and pore size distribution shown inset for a) Zn_2TiO_4, b) $Ag@Zn_2TiO_4$ and c) $Co@Zn_2TiO_4$

BET (Brunauer Emmett Teller) surface area (Table 1) of undoped Zn_2TiO_4 is found to be largest as compared to surface area of $Ag@Zn_2TiO_4$ and $Co@Zn_2TiO_4$. The larger pore volume and lower crystallite size of Zn_2TiO_4 may be responsible for high surface area. The FESEM and TEM images indicate depth of the pores is more in case of Zn_2TiO_4 as compared to Ag and Co doped Zn_2TiO_4. From the trend of pore volume and surface area, it can be concluded that porosity as well as surface area decreases due to doping. But BJH (Barrete-Joyner-Halenda) pore diameters are not in accordance with the BET pore diameter. This is because, BET method determines surface area of any shape and porosity while BJH assumes pores having cylindrical shape.[63,64] Hence, BET surface area and BET pore diameter are in agreement with each other. Plausible explanation regarding decrease in surface area may be given on the basis of morphology and crystallite size of pristine and doped zinc orthotitanates. Stacking of layers in case of $Ag@Zn_2TiO_4$ and compact cluster formation in case of $Co@Zn_2TiO_4$ as well as increase in crystallite size may also be the possible factors behind decrease in surface area. The phenomena of decrease in surface area upon doping have also been reported in previous studies.[56]

Table 1: BET Surface area, pore volume and pore diameter of zinc orthotitanates

Compound	BET (m^2/g)	Pore Volume cm^3/g (Pores < 77.1 nm)	Pore diameter (nm)
Zn_2TiO_4	12.24	0.040	13.1 (22.7)
$Ag@Zn_2TiO_4$	08.88	0.026	11.9 (30.8)
$Co@Zn_2TiO_4$	08.31	0.031	13.9 (29.5)

( ): BJH pore volume

3.6 Optical study

Optical characterization of the compounds synthesized was performed by UV-Vis DRS and Photoluminescence analyses. Fig. 11A represents the UV DRS spectra of Zn_2TiO_4 and Ag-doped Zn_2TiO_4 in absorbance mode and respective tauc plots (Fig. 11B). Band gap of the compounds has been determined form tauc plot.[65,66] Absorption edge of Zn_2TiO_4 appears to be at 385 nm and 335 nm with corresponding band gap 3.22 eV and 3.70 eV, respectively. Band gap observed for as synthesized Zn_2TiO_4 is higher than reported in literature (3.11 eV) indicates nanocrystalline nature.[37,68] In absorption spectra of Zn_2TiO_4 two absorption edges are observed which indicate existence of Zn_2TiO_4 in two phases. Band gap 3.22eV is attributed to tetragonal phase while 3.7 eV to cubic phase.[37]Many researchers synthesized Zn_2TiO_4 having tetragonal phase with band gap 3.11 eV and cubic phase with band gap 3.7 eV. [67-70] Absorption edge due ZnO (band gap 3.35 eV) has not been observed in the optical spectra. Band gap of Zn_2TiO_4 dominates band gap of ZnO when Zn/Ti ratio is 2 during synthesis of zinc orthotitantes.[68] In absorption spectra of $Ag@Zn_2TiO_4$, cut off observed at 387 nm is due to Zn_2TiO_4 while cut off at 738 nm is due to Ag nanoparticles with corresponding band gap 3.20 and 1.68 eV, respectively.

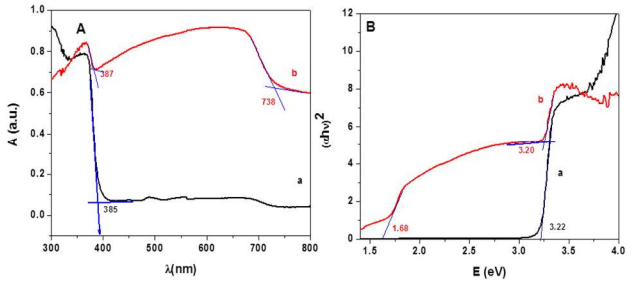

Fig.11 A) UV Vis -DRS absorption plot of Zn_2TiO_4 and $Ag@Zn_2TiO_4$ B) tauc plot of Zn_2TiO_4 and $Ag@Zn_2TiO_4$.

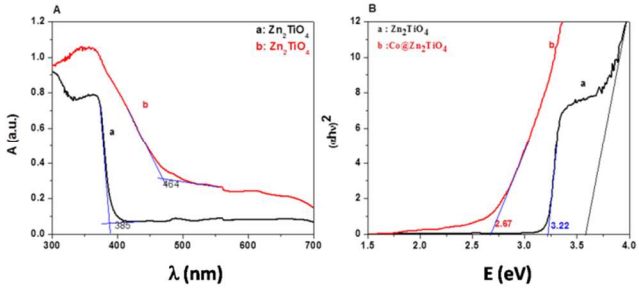

Fig. 12 A) UV vis-DRS of $Zn_2TiO_4$and Co@ Zn_2TiO_4 in absorbance mode and B) corresponding tauc plot

Fig. 12A represents UV vis DRS absorbance spectra of Zn_2TiO_4 and Co @Zn_2TiO_4 and Fig. 12B represents corresponding tauc plots. Optical spectra clearly show shifting of adsorption edge towards visible region at 2.67 eV due to Co doping. In general, absorption edge around 400 nm was ascribed to the band transition from O 2p to Zn 4s. In case of Co doped Zn_2TiO_4, new absorption edge has been observed at 2.67 eV. The absorption edge of Co doped Zn_2TiO_4 samples were based on transition from Co e_g to Co *4s* transition. In this case inter band may exist between the conduction and valence band of Zn_2TiO_4.[38]

The room temperature PL spectra of the Zn_2TiO_4(Fig. 13a) shows weak band at 330 nm, sharp strong peak at 363 nm and weak broad peak at 468 nm .The weak emission peak observed at 330 nm is because of band to band transition. This can be referred as near band edge emission which is closed to band gap observed at 335 nm in UV-Vis spectra .[71]

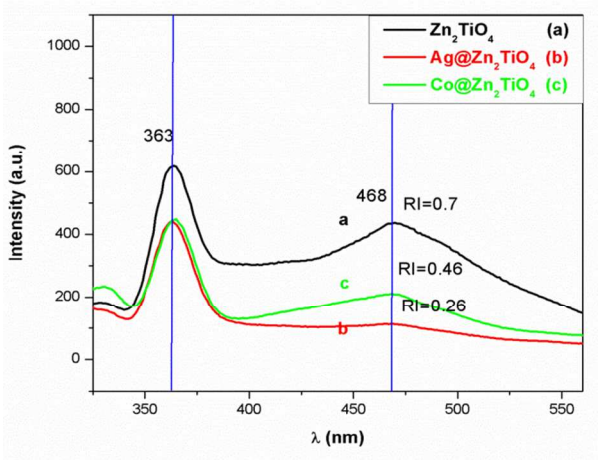

Fig.13 PL spectra of (a) Zn_2TiO_4 , (b)Ag@ Zn_2TiO_4 and (c) Co@ Zn_2TiO_4.

The emission peak observed at 468 nm indicates that defects exists in the crystalline ordered meso-structured Zn_2TiO_4.[72,73] The existence of intrinsic defects such as O^{-2} vacancies , Zn^{+2} vacancies may be responsible for such emission.[74] Ag and Co doping affects on the intensity of emission peaks observed at 468 nm. It is observed that relative intensity (RI) of peak at 468 nm (RI = 0.26) for $Ag@Zn_2TiO_4$(Fig. 13b**)** is lowest which shows complete diminishing of peak due to composite formation with Zn_2TiO_4. However, in case of Co@ Zn_2TiO_4 (Fig. 13c), it has been reduced to 0.46. It is well known that strong PL means high recombination of photo generated carriers suggesting low photocatalytic activity. Intensity of peak at 468 nm has been observed to be decreased due to Ag loading and Co(II) doping which decreases recombination probability and hence increases the photocatalytic activity. The decrease in intensity indicates minimization of lattice defects as compare to pristine Zn_2TiO_4.[75]

3.7 Photocatalytic H_2S splitting for H_2 generation

Photocatalytic splitting of H_2S can release the hydrogen by utilizing solar energy which is generally carried out in aqueous medium.[76, 85] Photocatalytic H_2S splitting has been performed using as synthesized nanostructured zinc orthotitanates. Amount of H_2 generated by using Zn_2TiO_4, Ag@ Zn_2TiO_4 and Co@ Zn_2TiO_4 with time under the visible light source is shown in the Fig. 14.

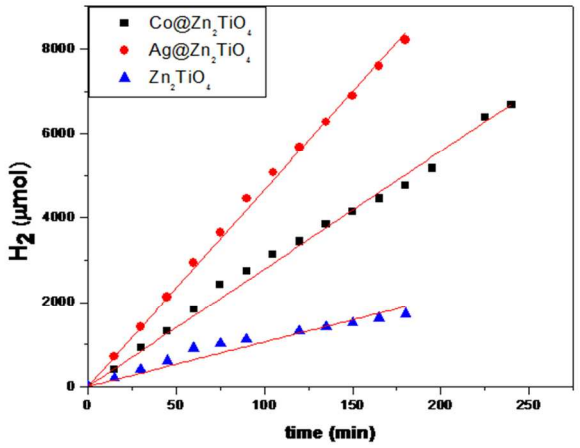

Fig. 14 Photocatalytic Hydrogen generation by using Zn_2TiO_4, Ag@ Zn_2TiO_4 and Co@ Zn_2TiO_4

Table 2: Rate of H_2 generation using zinc orthotitanates.

Sr. No.	Catalyst	Rate of H_2 generation (per 100 mg)	
		µmol /min	µmol /h
01	Zn_2TiO_4	10.55	633
02	Ag@ Zn_2TiO_4	46.40	2784
03	Co@ Zn_2TiO_4	27.87	1672

The H_2 evolution via H_2S splitting is given in the table 2. It reveals from literature that zinc orthotitanates have been employed for H_2S splitting to produce H_2 for the first time. The Zn_2TiO_4 showed H_2 evolution under visible light (633 µ mol/ h/100 mg) from H_2S. The naked zinc orthotitanate showed photocatalytic activity because of its high reduction potential and low oxidation potential and it is reported that it is better catalyst than TiO_2 under UV as well as visible light.[67,77] Amongst the zinc orthotitanates synthesized , Ag doped Zn_2TiO_4 has been found to be excellent photocatalyst. The utmost H_2 evolution (2784 µ mol /h /100 mg), under visible light irradiation was obtained which is much higher than H_2 produced using CdS, $CaIn_2S_4$, $CdLaS_4$, $ZnIn_2S_4$, N-ZnO , Fe_2O_3 and $FeGaO_3$.[19-26] (Table 3)

Table 3: Volume of H_2 evolved using various catalyst

Catalyst	Vol of H_2 generated / µmolh^{-1}	Ref.
Ag@Zn_2TiO_4	2784 (175 ml 0.25 N KOH, 0.1 g catalyst)	Present work
CdS	2945 (750 ml 0.25N KOH, 0.5 g catalyst)	26
$ZnIn_2S_4$	5287 (700 ml 0.25N KOH, 0.5 g catalyst)	23
$CdIn_2S_4$	3238 (750 ml 0.5N KOH, 0.5 g catalyst)	24
$ZnIn_2V_2O_9$	4695 (750 ml 0.5N KOH, 0.5 g catalyst)	20
$CdLaS_4$	2552 (250 ml 0.5N KOH, 0.5 g catalyst)	19
N-ZnO	3957 (200 ml 0.25N KOH,0.2 g catalyst)	25
Fe_2O_3	2038 (500 ml 0.5 N KOH,0.5 g catalyst)	22
$FeGaO_3$	2720 (250 ml 0.5M KOH, 0.5 g catalyst)	21

Enhanced photocatalytic activity of Ag@ Zn_2TiO_4 as compared to pristine Zn_2TiO_4 could be explained on the basis of Ag - Zn_2TiO_4 composite. Many researchers have reported that noble metal loading on the surface of the catalyst promotes the photocatalytic production of hydrogen.[85,78] Loaded metal can capture the photo generated electrons on the catalyst surface so that after excitation, the electrons are effectively separated from the holes and the life time of the electrons is prolonged. This increases the proportion of electrons that participate in photocatalytic reduction of protons to produce hydrogen.[64] On the other hand, hydrogen over potential of noble metal is very low. Loading metal on semiconductor can lower the electrochemical reductive potential ($E_{H^+/H2}$) which favours the photocatalytic hydrogen production. Additionally, the reason mentioned in dye degradation like plasmon resonance effect and broad absorption from 400-700 nm is also responsible for getting enhance photocatalytic activity. However, we obtained lower photocatalytic activity for Co@ Zn_2TiO_4(H_2 evolution @ 1672 µmol/h/ 100 mg) as compared to Ag@ Zn_2TiO_4.

As mentioned earlier, nature of the oxides formed is not same. Ag-Zn_2TiO_4 composite has been observed in the Ag@Zn_2TiO_4 while substitutional doping of Co^{+2} has been indicated in case of Co@Zn_2TiO_4 by XRD analysis. It is observed that not only surface area but also increase in recombination centre, extent of shifting of band gap towards visible region and composition of the catalyst affects on the efficiency of catalyst. In case of Co@ Zn_2TiO_4photocatalytic dye degradation efficiency was found to be decreased while photocatalytic H_2S splitting observed to be increased with respect to undoped zinc orthotitanates. It has been reported in the literature that $ZnCoTiO_4$ worked not only as an active site during sulfidation process but also as a support to prevent the Zn migration to the outside of the sorbents and to minimize the volume expansion / contraction. Hence doping of Co into Zn_2TiO_4 at the Zn site increases the efficiency of adsorption of H_2S on the surface compare to undoped Zn_2TiO_4 there by enhancement in H_2S splitting in presence of Co@ Zn_2TiO_4.

3.7.1 Mechanism of H_2 generation by H_2S splitting

Mechanism of H_2 generation by H_2S splitting under visible light source in basic medium has been mentioned by many researchers.[56,65,66]

It is well known that H_2S is a weak diprotic acid having pKa values 7.0 and 11.96 .[79] At pH ~13, dissociation of H_2S takes place to form HS^- and S^{-2}. When suspension irradiated with visible light, photocatalyst generates conduction band electron (e^-_{cB}) and valence band hole (h^+_{vB}). The detailed mechanism is given below.

$$H_2S + OH^- \leftrightarrow HS^- + H_2O \quad (2)$$

$$HS^- + OH^- \leftrightarrow S^{2-} + H_2O \quad (3)$$

$$ZOT + h\nu \rightarrow e^-_{cB} + h^+_{vB} \quad (4)$$

$$2S^{2-} + 2h^+_{vB} \rightarrow S_2^- \quad (5)$$

$$2HS^- + 2h^+_{vB} \rightarrow S_2^- + 2H^+ \quad (6)$$

$$2H^+ + 2e^-_{cB} \rightarrow H_2 \uparrow \quad (7)$$

Overall reaction is given below.

$$H_2S + 2OH^- - \frac{h\nu}{ZTO} \rightarrow H_2 + Polysulphide \qquad (8)$$

In nutshell, the orthotitanates are observed to be very stable oxide visible light active photocatalyst for hydrogen production as well as dye degradation. It is noteworthy that orthotitanates have been used for the hydrogen production from H_2S for the first time. Furthermore the degradation of azo dyes and xanthene dyes using orthotitanates under natural sunlight is hitherto unattempted.

3.8 Photocatalytic degradation of dyes

3.8.1 Photocatalytic degradation of Acid Orange-8 (AO-8)

Photocatalytic degradation of 40 ml aqueous solution having concentration 10 ppm using 10 mg photocatalyst was carried out under normal sunlight. The intensity of sun light has been measured using Lux meter and observed to be in the range 1.0 x 10^5 to 1.1 x 10^5 lux. (15- 15.5 eV) The graph of C/C_o(C_o : initial concentration of dye , C : concentration of dye at time 't') of the Vs time for Zn_2TiO_4, Ag@Zn_2TiO_4 and Co@Zn_2TiO_4 is shown in the Fig. 15. It is observed that photocatalytic activity increases due to Ag loading while decreases due to Co^{+2} doping into Zn_2TiO_4. Complete degradation takes place in ~ 75 min and 210 min using Ag -Zn_2TiO_4composite and pristine Zn_2TiO_4, respectively. In other words photocatalytic activity of Ag@Zn_2TiO_4 increases almost three times as compared to that of Zn_2TiO_4. Half life ($t_{1/2}$) period for the photocatalytic degradation was determined from graph of C/C_0Vs time and found to be 14.9 , 52.1 and 126.6 min for Ag@ Zn_2TiO_4, Zn_2TiO_4 and Co@Zn_2TiO_4, respectively. The degradation of AO-8 in absence of catalyst (blank) under sunlight has not been observed.

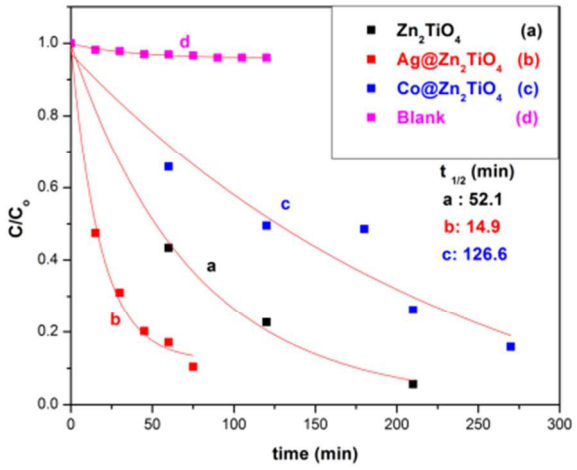

Fig. 15 Photocatalytic degradation of AO-8 using a) Ag@Zn_2TiO_4, b) Zn_2TiO_4 , c) Co@Zn_2TiO_4 and d) blank .

Since, photocatalytic activity of Ag@ Zn_2TiO_4 was found to be highest amongst the zinc orthotitanates synthesized, it has been chosen for the detailed study. Effect of concentration of AO-8 and amount of catalyst on the rate of degradation was studied for the Ag@ Zn_2TiO_4.

Effect of concentration of AO-8 was studied at 5, 7.5 and 10 ppm concentrations (Fig.16). Half life period determined from the graph was found to be 14.9, 22.0 and 57.0 min for 5, 7.5 and 10 ppm solutions, respectively.

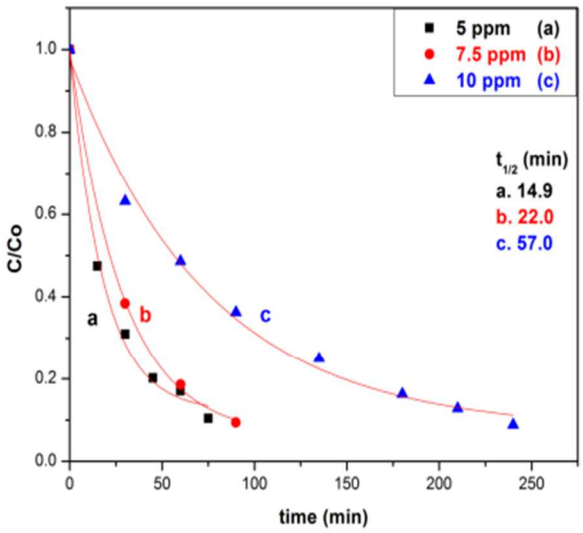

Fig. 16 Effect of concentration of AO-8 a) 5 b) 7.5 and c) 10 ppm

It is observed that, reaction time increases with increase in concentration of AO-8. Half life period ($t_{1/2}$) for 5, 7.5 and 10 ppm was found to be 14.9, 22.0 and 57.0 min, which show that $t_{1/2}$ is directly proportional to the concentration of the AO-8. Effect of the concentration of the catalyst on the rate of the reaction has been studied by taking 10, 20 and 30 mg Ag@ Zn_2TiO_4. (ESI, S-6) indicates reaction time decreases with amount of the catalyst. Half life period ($t_{1/2}$) is observed to be 14.9, 9.6 and 8.3 min for 10, 20 and 30 mg catalyst, respectively. Decrease in half life period ($t_{1/2}$) with amount of the catalyst also indicates that the rate of reaction increases with amount of the catalyst. In other words, rate of photocatalytic degradation increases with increase in amount of the catalyst.

Decrease in half life period with increase in amount of the catalyst is quite obvious since rate of the reaction depends upon extent of the adsorption which in turn depends on the amount of the catalyst.

3.8.2 Photocatalytic degradation of Rhodamine B (Rh-B)

The as synthesized nanostructured zinc orthotitanates were also employed for the photocatalytic degradation of Rh- B dye in aqueous medium. Variation of C/C_o with time of the reaction for 5 ppm solution using 10 mg catalyst is shown in the Fig. 17, which shows similar behaviour observed in case of AO-8. There is negligible decrease in concentration of the Rh-B in absence of catalyst (blank) indicates no degradation due to photolysis.

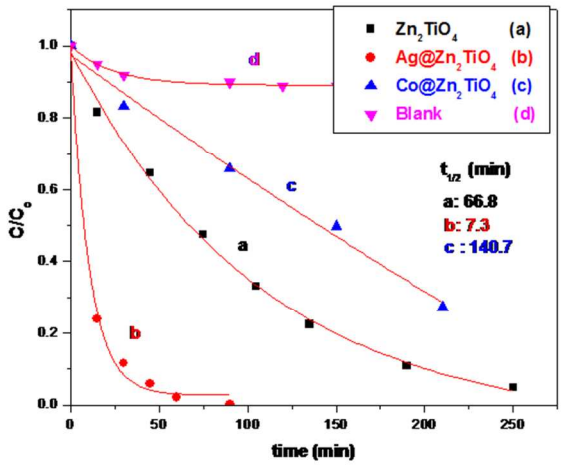

Fig. 17 Photocatalytic degradation of Rh- B using a) $Ag@Zn_2TiO_4$, b) Zn_2TiO_4 c) $Co@Zn_2TiO_4$ and d) blank

Effect of concentration of the Rh- B on the rate of photocatalytic degradation was studied at 2.5, 5.0 and 7.5 ppm Rh-B solution using 10 mg $Ag@ Zn_2TiO_4$. The variation of C/C_o with time is shown in the Fig. 18. Half life period ($t_{1/2}$) determined from the graph was found to be 4.4, 7.3 and 13.2 min for 2.5, 5.0 and 7.5 ppm, respectively. In this case, rate of photocatalytic degradation also decreases with increase in concentration of the Rh-B.

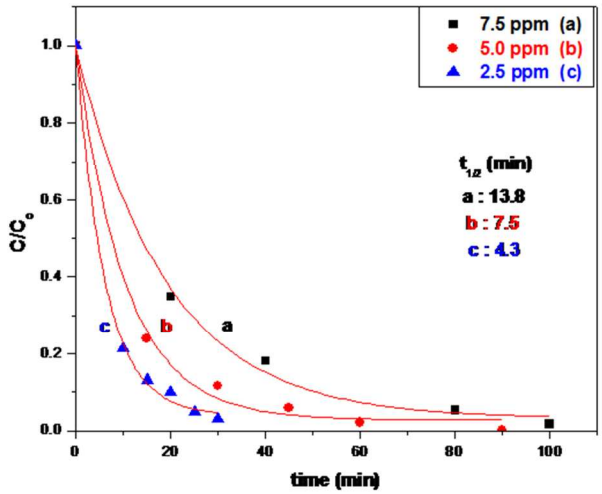

Fig. 18 Effect of Concentration of RH- B a) 2.5 b) 5 c) 7.5 ppm solution.

Effect of the amount of catalyst on rate of photocatalytic degradation was studied for 10 and 20 mg catalyst for 5 ppm solution and 20 and 30 mg catalyst for 7.5 ppm (ESI S-7) solution. The effect of amount of catalyst has been studied for 7.5 ppm in addition to 5 ppm solution since degradation of 5 ppm solution using 30 mg photocatalyst was too fast to measure rate of reaction.

Rate of photocatalytic degradation observed to be increases with amount of the catalyst. Half life period ($t_{1/2}$) determined was 7.4 and 3.6 min for 10 and 20 mg catalyst, respectively for 5 ppm solution while, 4.2 and 2.8 min for 20 and 30 mg catalyst, respectively for 7.5 ppm concentration of Rh-B (ESI, S-7).

The enhancement in degradation rate can be rationalized in terms of available active sites and penetration of photo activating light into the suspension. The availability of active site increases with increase in concentration of catalyst up to certain limit. Because, at high concentration of catalyst, i) light penetration decreases which affect photo activated volume of suspension ii) deactivation of activated catalyst molecule due to collision with ground state molecules(**Eq. 9**) . Hence, decrease in rate of degradation at higher concentration of catalyst is quite justifiable.[80]

$$ZOT^* + ZOT \rightarrow ZOT^{\#} + ZOT \quad (9)$$

Where * and # represents activated and deactivated molecule of zinc orthotitanate (ZOT) respectively.

Therefore, an optimum amount should be employed to ensure the utmost absorption of solar light photons for efficient photo mineralization.[29] It is observed that degradation rate decreases with increase in concentration of dye. As initial concentration of dye increases, the path length of the photon entering the solution decreases and at low concentration reverse effect is observed thereby increasing photon absorption by the catalyst.[36,81] It is quite obvious that, as the initial concentration of dye increases, requirement of catalyst surface needed for the degradation also increases. Since amount of catalyst is fixed, the formation of $OH^{\cdot}$ radicals on the surface of zinc orthotitanate is also relatively fixed. So the relative number of free radicals attacking the dye molecule decreases with increase in concentration of dye.[82] The major portion of degradation occurs in the region (reacting zone) near to the irradiated sites because the irradiation intensity in this region is much higher than at the other sites.[83] Hence, at higher concentration of dye, there is decrease in rate of degradation. [80]

A photocatalytic process is based on the generation of electron hole pair by means of band gap radiation that can give rise to redox reaction with the species adsorbed on the surface of the catalyst. In principle, the coupling of different semiconductor oxides seems useful in order to achieve more efficient electron pair separation under irradiation and consequently the higher photocatalytic activity.[36] It is reported that absolute pure phase Zn_2TiO_4 is photocatalytically inactive however coupling of Zn_2TiO_4 with ZnO shows an enhancement in photocatalytic activity. *Cunwang et.al.* reported that photocatalytic activity towards degradation of methyl orange was observed for Zn_2TiO_4-ZnO composite and not for pure phase Zn_2TiO_4.[36] In our case Zn_2TiO_4 synthesized shows photocatalytic activity towards degradation of AO-8 and Rh-B. The existence of zinc orthotitanate in tetragonal phase having band gap at ~ 3.2 eV is responsible for photocatalytic activity. In earlier studies *Borse et al.* reported photocatalytic activity of Zn_2TiO_4 having band gap 3.11 eV.[77] The existence of ZnO along with Zn_2TiO_4 may be also responsible for its photocatalytic activity.

Enhancement in photocatalytic degradation activity of dyes using $Ag@ Zn_2TiO_4$ with respect to undoped Zn_2TiO_4 is due to Ag metal loading on the surface of the Zn_2TiO_4 which promotes the photocatalytic degradation of dyes.[76,84,85] Enhancement in photocatalytic activity due to Ag nanoparticles is because of i) additional band gap observed at 1.62 eV with broad absorption in the visible region 400- 700 nm ii) promotion of visible light absorption through surface plasmon resonance of Ag nanoparticles iii) Ability of silver to reduce the recombination by trapping of electrons through introduction of Fermi level of

silver which is just below the conduction band of Zn_2TiO_4.[86,87]

The rate of degradation of AO-8 and Rh-B is decreased in case of Co@ Zn_2TiO_4 despite shift in band gap towards the visible region (~ 2.7 eV). Surprisingly, it is much less as compared to undoped Zn_2TiO_4. This decrease is may be due to induction of recombination site because of doping of Co^{+2} ions into Zn_2TiO_4. In the case of Co^{+2} doping, induction of recombination sites is more dominant under the solar irradiation. Since intensity of the sun light is not enough to separate the electron hole pair, so recombination increase thereby decrease in rate of degradation.[88]

3.8.3 Photocatalytic degradation of mixture of dyes

Photocatalytic degradation of mixture of AO-8 (5.0 ppm) and Rh-B (5.0 ppm) was performed using 10 mg of Ag@ Zn_2TiO_4. These two dyes are not reacting with each other and hence their degradation in mixed state was performed. Graph of variation of C/C_0 with time is shown in the Fig. 19. It's observed that in mixture state, degradation rate of Rh-B is higher than AO-8. It means trend is same as observed in case of individual dyes.

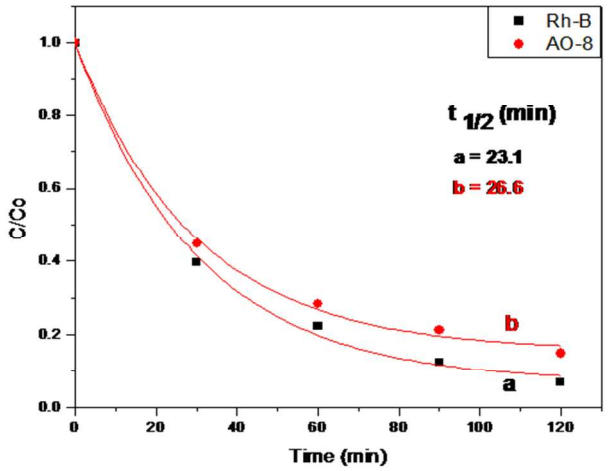

Fig. 19 Photocatalytic degradation of mixture of dyes: a) Rh-B, b) AO-8

From the half life period of degradation of dyes in individual and mixed state, it is clear that rate of degradation of the dyes has been decreased (Table 4). This is quite obvious because total concentration of the dye has been increased to 10 ppm. In mixed state, degradation of dye takes place in presence of other dye molecules which affects on rate of the reaction.

Table 4: Order and half life period of AO-8 and Rh-B

Sr. No.	Dye	Order (n)		Half life period ($t_{1/2}$) (min)	
		Individual	mixed	Individual	mixed
01	AO-8	1.35	1.41	14.9	26.6
02	Rh-B	1.10	1.25	7.5	23.1

Marginal increase in order of reaction has been observed with respect to individual state. This indicates that Ag@Zn_2TiO_4 can be employed for photocatalytic degradation of mixed dyes. The mixture of dyes affects on i) extent of light transmitted through solution and incident on surface of the catalyst, ii) number of water molecules adsorbed and dissociated to form active species like $OH^{\cdot}$ and O_2^- iii) distribution of the active species amongst the dye molecules. These factors are responsible for the decrease in rate of the degradation.

Study of degradation of dyes in mixed state is essential in practical point of view, because effluent may comprise variety of pollutants. These pollutants should be degraded simultaneously by photocatalyst. Thus, the Ag@ Zn_2TiO_4 can be employed effectively for degradation of mixed dyes. It is noteworthy that such type of study has been performed for the first time.

3.9 Kinetics study

Kinetics of photocatalytic degradation of organic dyes under UV and visible light has been studied by many researchers. It was reported that photocatalytic degradation follows first order kinetics based on Langmuir-Hinshelwood Model.[89,90] We have also performed kinetics calculation considering the photocatalytic dye degradation obeying pseudo first order kinetics as per Langmuir-Hinshelwood Model. In case of photocatalytic degradation of AO-8 and Rh-B, it is observed that extent of the degradation of the dye (C/C_0) decreases with increase in concentration of the dye. In other words, half life period of the reaction increases with increase in concentration of the dye. As per the characteristics of the first order reactions, half life period is independent of the initial concentration of the reactant (Dye) according to equation 10.

$$t_{1/2} = \frac{0.693}{k_1} \qquad (10)$$

Our observation indicates the discrepancy between rate constant and order of the reaction. *D Zhang et. al*, reported that the discrepancy between first order reaction and rate constant may arise due to complicated mechanism.[91] The complicated mechanism would be influenced by many factors such as particle size, phase and chemical composition, surface properties, intensity of light and effectiveness of charge separation.

To investigate the apparent order of the reaction, we have assumed that photocatalytic degradation of dye takes place in the solution phase and not on the surface of the catalyst. So, we have used power rate law to determine the order of the reaction. The power rate law can be applied for homogenous reactions. [92]

Kinetics of the photocatalytic degradation has been studied using equation 11, which is applicable for the reaction of single reactant (A → Product)

$$Rate = -\frac{dC}{dt} = KC^n \qquad (11)$$

Where C, n and K are concentration of the reactant at time t, order of the reaction and rate constant of the reaction, respectively. Order and rate constant of the reaction can be determined from the logarithmic form of the equation 12.

$$\log(R) = \log K + n\log(C) \qquad (12)$$

Slope and intercept of the graph of log (R) Vs log (C) gives order (n) and rate constant (k) of the reaction.

Expression for half life period of the n^{th} order reaction has been derived from equation 11.

$$(t_{1/2})_n = \frac{\left(\frac{Co}{2}\right)^{1-n}}{k_n(1-n)}[2^{1-n} - 1] \qquad (13)$$

Where, K_n is the rate constant of the n^{th} order reaction and C_o is the initial concentration. Equation (13) is not applicable for n=1. The exercise to determine the order and rate constant of the reaction is illustrated for the photocatalytic degradation of the 40 ml 5 ppm solution of AO-8 using 10 mg Ag@ Zn_2TiO_4 catalyst. Variation of log (R) with log (C) is shown in the Figure 20.

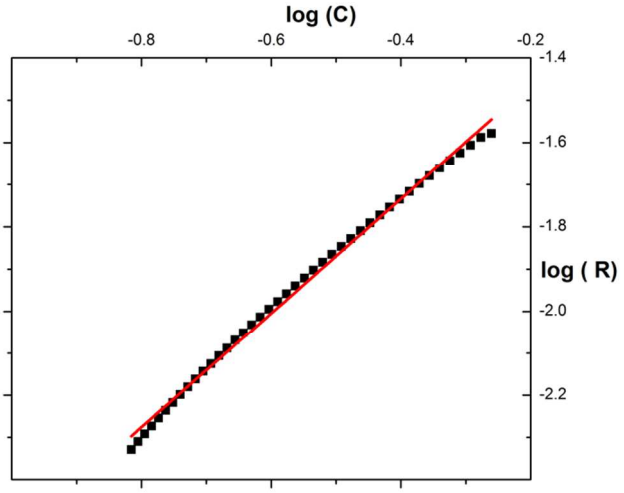

Fig.20 Graph of log (R) Vs log (C) for the 5 ppm solution of AO-8 using 10 mg Ag@Zn_2TiO_4.

Half life period and rate constant calculated from interpreted order of the reaction, first order kinetics and experimental observations are given in Table No. 5 and 6 for AO-8 and Rh-B solution.

Table 5: Kinetic parameters of photocatalytic degradation of AO-8 using Ag@Zn_2TiO_4

Conc. of dye (ppm)	Conc. of catalyst (mg)	Order (n)	Rate Constant		Half life period ($t_{1/2}$) (min)		
			K_n (conc^{1-n} min^{-1})	K_1 min^{-1}	n^{th} order	1^{st} order	Obs.
05.0	10	1.35	0.064	0.032	15.0	21.7	14.9
07.5		1.30	0.038	0.027	22.5	25.5	22.0
10.0		1.22	0.013	0.010	58.1	68.2	57.0
05.0	20	1.41	0.108	0.048	09.6	14.5	09.6
05.0	30	1.40	0.124	0.068	08.1	10.1	08.3

Order of the reaction was found to be in the range 1.2 – 1.41 for AO-8 and 1.1-1.2 for Rh-B. Experimentally determined rate constant and half life period of the reaction indicates that rate constant of reaction decreases with increase in concentration from 2.5 to 7.5 ppm. Dependence of the rate constant of the reaction on the initial concentration of the reactant is characteristic property of the reaction having order higher than one. It is observed that half life period calculated from equation and from experimental observation i.e. graph of C/C_o Vs time is in good agreement with each other. While, half life period calculated from first order kinetics is not in agreement with experimental value.

Table 6: Kinetic parameters of photocatalytic degradation of Rh-B using Ag@Zn_2TiO_4

Conc. of dye (ppm)	Conc. of catalyst (mg)	Order (n)	Rate Constant		Half life period ($t_{1/2}$) (min)		
			K_n (conc^{1-n} min^{-1})	n^{th} order	n^{th} order	1^{st} order	Obs.
02.5	10	1.20	0.190	0.121	04.4	05.8	04.3
05.0		1.10	0.096	0.067	07.4	10.4	07.5
07.5		1.20	0.052	0.040	13.2	17.4	13.8
05.0	20	1.16	0.202	0.160	03.6	04.3	03.8
07.5	30	1.14	0.238	0.168	02.8	04.1	03.0
07.5	20	1.16	0.159	0.108	04.2	06.4	04.3

3.9.1 Mechanism of the photocatalytic degradation

From experimental observation, it is proposed that water is adsorbed on the surface of the catalyst followed by formation of $OH\cdot$ and O_2^- radicals due to redox reaction taking place by photo excitation of electron under the sunlight irradiation. These photo generated radicals react with the dye molecule in solution state and degradation takes place. In the review article on TiO_2 assisted photocatalytic degradation of azo dyes in aqueous solution demonstrated the mechanism which involves formation $OH\cdot$ and O_2^- radicals.[91,93,94] Mechanism of photocatalytic degradation of dye is given below.

$$Zn_2TiO_4 + hv \rightarrow Zn_2TiO_4\,(e_{CB}^- + h_{VB}^+) \qquad (14)$$

$$H_2O + h_{VB}^+ \rightarrow OH\cdot + H^+ \qquad (15)$$

$$O_2 + e_{CB}^- \rightarrow O_2^- \qquad (16)$$

$$OH\cdot + dye \rightarrow H_2O + CO_2 \qquad (17)$$

$$O_2^- + H\cdot \rightarrow OOH\cdot \qquad (18)$$

$$OOH\cdot + OOH\cdot \rightarrow H_2O_2 + O_2 \qquad (19)$$

$$O_2^- + \text{Dye} \rightarrow CO_2 + H_2O \qquad (20)$$

$$OOH\cdot + \text{dye} \rightarrow CO_2 + H_2 \qquad (21)$$

In nut shell, the higher photocatalytic activity has been obtained for Ag@ Zn_2TiO_4 as compared to pristine Zn_2TiO_4 and Co@ Zn_2TiO_4. The kinetic study showed the dye degradation follows order of reaction in the range 1.1-1.4 with optimum concentration 2.5 -7.5 ppm

4 Conclusions

We have demonstrated the synthesis of nanostructured Zn_2TiO_4 , Ag@Zn_2TiO_4 and Co@Zn_2TiO_4 by combustion method . The structural properties showed cubic and tetragonal mixed phases of zinc orthotitanate. The particle size was observed to be in the range of 10-25 nm. The optical properties showed that band gap can be tuned with Ag and Co to the visible region i.e. from 3.22 to 1.67 eV. Considering the band gap in visible region, the photocatalytic activity of dye degradation (individual and mixed) under natural sun light has been performed with kinetic study. The Ag@Zn_2TiO_4 was found to be most efficient photocatalyst. The power rate law for n th order reaction in homogenous medium

has been employed to determine order (n), rate constant (k) and half life period ($t_{1/2}$).The order of the reaction observed to be in the range of 1.1-1.41 for AO-8 and Rh–B. Half life period calculated from order and rate constant was observed to be in good agreement with experimental values. The solar photo hydrogen production was also performed using undoped and doped ZOT. It is noteworthy that utmost hydrogen production (2784 µmol/h/100 mg) was obtained using $Ag@Zn_2TiO_4$ which is much higher than the oxide photocatalyst reported so far. This catalyst may have good potential in water splitting and complex waste degradation.

Acknowledgements

The authors are are thankful to Centre for Materials for Elelctronics Technology (C-MET), Pune and Department of Electronics and Information Technology(DeitY), New Delhi for financial support. We are also grateful to Principal, B. G. College, Sangvi, Pune for support.

Notes and references

a. *Centre for Materials for Electronics Technology (C-MET), Department of Electronics and Information Technology(DeitY), Pune, Maharashtra (India), Pin-411008.kbbb1@yahoo.com ; bbkale@cmet.gov.in*

b. *Baburaoji Gholap College, Sangvi, Pune, Maharashtra (India), Pin-411008,*

† Electronic Supplementary Information (ESI) available: ESI includes JCPDS data ,FTIR graphs,EDXRF analyses, ED pattern of $Ag@Zn_2TiO_4$, polar volume plots and kinetcs plots of dyedegradation

.

1 A .C. Chavez, S.J.G. Lima, R.C.M.U. Araujo, M.A.M.A. Maurera, E. Longo, P.S. Pizani, L.G.P. Simoes, L.E.B. Soledade, A.G. Souza and I.M.G. Dos Santos, *J. Solid State Chem.,* 2006,**179**, 985.

2 T. Ivanova , A. Harizanova , T. Koutzarova and B. Vertruyen, *J. Non-Cryst.Solids*, 2011, **357**,2840.

3 M. L. Levy, *Compt. Rend*., 1888, **107**,421 .

4 F. Bartram and R. A. Slepetys, *J. Am. Ceram. Soc.,* 1961,**44**,493.

5 M.Yamaguchi, H. Morimi, Kawabata, and K. Shimizu, J. Am. Ceram. Soc., 1987, 70 (5) ,C-97–C-98.

6 Steinike and B. Wallis, *Cryst. Res. Technol*., 1997, **32**,187.

7 X.C. Liu, F. Gao, L.L. Zhao,and C.S. Tian, *J. Alloys Compd*., 2007, **436,**285.

8 Y. Zheng, V. Zhao,W. Lei, and S.Wang, *Mater. Lett.,* 2006 , **60,**459.

9 J. Zhu, E.R. Kipkoech and W. Lu, *J. Eur. Soc.,* 2006, **26,**2027.

10 N. Obradovic, N. Labus, T. Sreckovic, D. Minic, and M.M. Ristic, *Science and Sintering,* 2005, **37**,123.

11 H. T. Kim, J. D. Byun, and Y. Kim, , *Mater. Res. Bull*., 1998, **33**, 963.

12 C. Siriwong, N. Tamakeong, and S. Phanichphant, *Material letters,* , **2012**, *68*, 97.

13 J. Mrazek, L. Spanel, M. Surynek, M. Potel, and V. Matejec, *J. Alloys and compound*, 2011, **509,**4018.

14 S. Butee, A. R. Kulkarni, O. Prakash, R.P.R.C. Aiyar, I. Wattamwar, D. Bais, K. Sudheendran and K.C. James Raju, *Materials Science and Engineering B*,2011, **176,**567.

15 S. C. Souza, M. A. F. Souza, S. J. G. Lima, M. R. Cassia-Santos, V. J. Fernandes Jr., L. E. B. Soledade, E. Longo, A. G. Souza and I. M. G. Santos, *Journal of Thermal Analysis and Calorimetry*, 2005, **79,**455.

16 E. Shoko, B. McLellan, A.L. Dicks, and J.C.D. da Costa, *Int. J. Coal Geol*., 2006, **65,** 213.

17 E. Sasaoka, *Energy Fuel*, 1994, **8**,763.

18 S. Hao , R. B. Rankin , J. K. Johnson and D. S. Sholl, *Surface Science*, 2011, **605,** 818.

19 B. B. Kale, J. O. Baeg, K. J Kong, S.J. Moon, L. K. Nikam and K. R. Patil, *J. Mater. Chem.*, 2011, **21**,2624.

20 S. A. Mahapure, J. D. Ambekar, L. K. Nikam, R. Marimuthu, M. V. Kulkarni, and B. B. Kale, *J.Nanosciand Nanotechnol,* 2011, **11**,1.

21 E. Subramanian, J.O. Baeg, S. M. Lee, S.J. Moon and K.J. Kong , *Int. J.Hydrogen Energ*, **2008**, *33*,6586

22 S. K. Apte, S. D. Naik, R. S. Sonawane, B. B. Kale and J. O. Beag, *J. Am. Ceram. Soc.* 2007, **90(2),** 412

23 N. S. Chaudhari, A. P. Bhirud, L. K. Nikam, S. S. Warule, R. S. Sonawane, V S.Rane, J. O. Beag and B. B.Kale*Green Chem*., 2011, **13,** 2500.

24 A. Bhirud , N. Chaudhari , L. K. Nikam , R. Sonawane , K. Patil , J. O. Baeg and B. B. Kale *Int.J. hydrogen energ,* 2011, **36,** 11628.

25 A.P. Bhirud, S. D. Sathe, R.P. waichal, L. K. Nikam and B. B. Kale,*Green Chem.* 2012,**14**,2790.

26 S. K. Apte, S. N.Garaje, G. P. Mane, A. Vinu, S. D. Naik, D. P. Amalnerkar and B. B. Kale, *Small*, 2011,**7,** 957.

27 C. Bauer., P..Jacques and A. Kalt., *J. Photochem. Photobiol. A: Chemistry*, 2001,**140,**87.

28 P. Mehta, R. Mehta, M. Surana and B.V. Kabra. *J. Ind. Council Chem.*, 2009, 26(2),158.

29 R. Jain,. M.,Mathur, S.Sikarwar, and A.Mittal, *J. Environ. Manag*. 2007, **85**,956.

30 M. Mrowetz, C. Pirola, andE. Selli, *Ultrasonics Sonochemistry*, 2003, **10**,247.

31 S. M. Lam , J.-C. Sin , A. Z. Abdullah and A. R. Mohamed, *Desalination and Water Treatment*, 2012, **41,**131.

32 L. Jing-yi, M.A. Wan-hong, L. Peng-xiang, and Z. Jin-cai, *Journal of Environmental Sciences*,2007, **19,** 892.

33 R. Mehta and M. Surana, , *Der Pharma Chemica*, 2012, **4(1),**311.

34 P.Bingcai, X. Yingmei, Z. Shujuan, L.Lu, and Z. Weiming, *ACS Appl. Mater. Interfaces*, 2012, **4**, 3938.

35 G.Ming, L. Lu, C. Wei and Z. Zhen , *Cryst Eng Comm*, 2012, **14,**1038.

36 C. Wang, B. Xu, X. Wang, and J. Zhao, *Journal of Solid State Chemistry* ,2005, **178,**3500.

37 S.A. Maye´n-Herna´ ndez, G. Torres-Delgado, R. Castanedo-Pe´rez, J. Ma´ rquez Marı´n, M. Gutie´rrez-Villarreal, and O. Zelaya-Angel, *Solar Energy Materials & Solar Cells*, 2007, **91**,1454.

38 L. Wan, X. Li , Z. Qu, Y. Shi, H. Li , Q. Zhaoa and G. Chen , *Journal of Hazardous Materials*, 2010, **184**, 864.

39 (a) J. S. Jang, P. H. Borse, J. S. Lee, K. T. Lim, O.S. Jung, E. D. Jeong, J. S. Bae, M. S. Won, and H. G. Kim, *Bull. Korean Chem. Soc.* 2009, **30 (12),**3021; (b) L. K. Nikam , R. Patil , R. Panmand , S. Kadam, K. Sivanandan and B. Kale , *Adv Sci Eng, Med.* 2013,**5 (7),** 688.

40 S Vivekanandhan, M Venkateswarulu, and N.Satyanarayana *Mater Chem Phys* 2008, **109**,141.

41 K. C. Patil , S.T. Aruna, and T. Mimani, *Current Opinion in Solid State and Materials Science* 2002, *6*,507.

42 R. L Millard, and R. C Pitterson , *American mineralogist*, **1**995**, 80**, 885.

43 S.J. Marin, M. O'Keeffe and D.E. Partin, *J solid state chem.*, 1994, *1***13,**413.

44 C. Li, Y. Bando, M. Nakamura, N. Kimizuka and H. Kito , *Materials Research Bulletin*,2000, **35***,* 351.

45 K.C. Patil , S T. Aruna: A. A Borisov, L.T.De Luca, A.G. Merzhanov, Y.N. Scheck, editors., *Redox methods in SHS practice in self-propagating high temperature synthesis of materials,*'. New York: Taylor & Francis; 2002

46 T V Anuradha and S Rangnathan, *Bull. Mater. Sci*. 2007, **30(3),**263.

47 PCPDFWIN, JCPDS card No. 86-0158 (1997)

48 PCPDFWIN JCPDS card no. 86-154 (1997)

49 N. T. Nolan, M. K. Seery, and S. C. Pillai, , *Chem. Mater*. 2011, **23**, 1496.

50 PCPDFWIN, JCPDS card No 04-783 (1997)

51 PCPDFWIN, JCPDS card No. 89-1397(1997)

52 M. Umadeviand A. Jegatha Christy,*Spectrochimica Acta Part A: Molecular and Biomolecular Spectroscopy,* (in press) **2013**, DOI 10.1016/j.bbr.2011.03.031.

53 X. M. Wu, S. Chen, Z.Q. He, Z. B. Xiao, M. Y. Ma, J. B. Liu, *Ceramics International*. 2008, ***34 (6)***, 1387.

54 T. Morita, Y. Yasuda, E. Ide , Y.Akada and A. Hirose, *Materials Transactions,* 2008,***49(12),***2875 .

55 R. D. Shannon, *Acta Crystallographica* ,1976. ***A32***, 751

56 H. K. Jun, T. J. Lee, S. O. Ryu, and J. C. Kim, *Ind. Eng. Chem. Res*., 2001, ***40***,3547.

57 M.R. Mohammadi and D. J. Fray, *J European ceramic soc* 2010, ***30(4),***947.

58 R. Iordanova, A. Bachvarova-Nedelcheva, Y. Dimitriev, and T.. Iliev, *Bulgarian Chemical Communications*, 2011, ***43,*** 378.

59 V.A.M. Brabers, *Phys. State. Sol*. 1972, ***12,***629.

60 L. G. Devi, B. Nagaraj, and K. E.Rajashekhar, *Chemical Engineering Journal* , 2012, **181– 182,** 259.

61 J. García-Serrano, E. Gómez-Hernández , M. Ocampo-Fernández and U. Pal, *Current Applied Physics,* 2009, **9**,1097.

62 K. S. W. Sing, D. H. Everett, R. A. W. Haul, L. Moscou, R. A. Pierotti, J. Rouquerol and T. Siemieniewska, *Pure Appl. Chem.*, **1**985, ***57(4),***603.

63 E. P Barrett , *J. Am. Chem. Soc*. 1951, ***73,*** 373.

64 O.M.Poltorak, *Thermodynamics in Physical Chemistry*. (Moscow: Vysshajashkola), 1991. 319 .

65 A. E. Morales, E. S´anchez Mora, and U. Pal,*Revista Mexicana Defisica S*, **53(5)**, 18.

66 R.A. Smith, *Semiconductors*, 2nd ed. , Cambridge University Press: Cambridge, 1978 .

67 Matsumoto, Y. *J. Solid State Chem.*, **1**996, **126**,227

68 S. A.Maye´n-Herna´ndez, G.Torres-Delgado, R..Castanedo-Pe´rez, M. G.Villarreal,A.Cruz-Orea,; J. G. M.Alvarez and O.Zelaya-Angel, *J. Mater. Sci.: Mater.* El., 2007,**18 (11),**1127.

69 J. Mra´zek, L. Spanhel, G. Chadeyron, and V. Mateˇjec, *J. Phys. Chem. C,* 2010, **114,** 2843.

70 G. Krylova, A. Brioude, S. A. Girard, J. Mrazek and L. Spanhel, *Phys. Chem. Chem. Phys*. 2010, **12**,15101.

71 S.Y. Pung,W. P. Lee, and A. Aziz,*International, Journal of Inorganic Chemistry*,2012, Article ID 608183

72 L. S Cavalcantea,. M. F. C Gurgel, A. Z Sim~oes,. E .Longo,.; J. A.Varela,M. R Joya and P. S Pizani,. *Appl. Phys. Lett.,* 2007, **90,**011901.

73 J Ni,. Q. Zhou, Z. Li, and Z.Zhang, *Appl. Phys. Lett***.**2008, **93,** 011905.

74 C. Ye, Y. Wang, Y. Ye, J. Zhang,and G.H. Li, *J. Appl. Phys*. 2009, **106,**033520

75 (a)Y.M. Chiang, D.P. Birnie III, and W.D. Kingery, *Physical Ceramics— Principles for Ceramic Science and Engineering,* Wiley, New York, 1997. (b) D.Chen, Z. Wang, T. Ren, H. Ding, W. Yao, R. Zong, and Y. Zhu, *J. Phys. Chem. C* 2014, **118**, 15300.

76 Z. B Lei, W S.You, M. Y Liu, G H Zhou, T Takata, M Hara, K Domen and C. Li. *Chem. Commun*., 2003, **17**,2142

77 P. H. Borse, C. R. Cho, K. T. Lim, T. E. Hong, E. D. Jeong, J. H. Yoon, S. M. Yu and H. G. Kim, *Journal of Ceramic Processing Research*. 2012,42.

78 Wu Y. *Catalysis Chemistry*. Beijing: Science Press, **2000**. 1345.

79 J. A Navio,.G, Colon,. M. I.Litter and G. NBianco, *J. Mol. Catal. A: Chem,*1996,**16**, 267.

80 B. Neppolian , H.C. Choi , S. Sakthivel, B. Arabindoo , and V. Murugesan, *Journal of Hazard. Mater.***2002**, *B89***,** 303.

81 B.Tryba, P.Brożek, M.Piszcz, and A.W.Morawski, *Pol. J. Chem. Tech*., 2011, **13(4),** 8.

82 A. R.Bally,E. N. Korobeinikova, P. E Schmid,. F.Levi, F Bussy,. *J. Phys. D: Appl. Phys*.,1998,**31,**1149

83 E.Borgarello.; J.Kiwi; M.Gratzel, E. Pelizzetti,and M..Visca, *J. Am. Chem. Soc*. 1982, **104,** 2996.

84 N Bao, L Shen, T Takata, K Domen, A Gupta, K Yanagisawa and, C A Grimes. *J Phys Chem C*, 2007, **111(47),** 17527

85 T Chen, Z. C. Feng, G P Wu, J Y Shi, G J Ma, P L Ying, C..Li ,*J Phys Chem C*, 2007, **111(22),**8005

86 M. K Seery; R.George, P.Floris and S. C..Pillai, *J. Photochem. Photobiol. A,* , 2007, **189,**258

87 C..Gunawan, W. Y.Teoh, Marquis and C. P.; Lifia, *J. Amal, R. Small* , 2009, **5**,341

88 D. Bahnemann, in: P. Boule (Ed.), *Photocatalytic degradation of polluted waters, The Handbook of Environmental Chemistry.* 2. Part L: Environmental Photochemistry,Springer, Berlin, 1999, 285–351.

89 I. K. Konstantinou, T. A. Albanis, *Appl Catal B: Environ*, 2004, **49,** 1.

90 S.M. Lam , J.C. Sin , A. Z. Abdullah and A. R. Mohamed, *Desalination and Water Treatment*, **2**012, **41,** 131.

91 D. Zhang, Pol. J. Chem. Tech., **2**012,*14(2),* 42

92 C. H. Wu and J. M. Chern , *Ind. Eng. Chem. Res*., **2006**, **45,** 6450.

93 L. Wang, L. Chang, B. Zhao, Z. Yuan, G. Shao, and W. Zheng, , *Inorg Chem*, 2008, **47 (5),** 1443.

94 J. H. Zeng, B. B. Jin, and Y. F. Wang, *Chem Phys Lett*, 2009,**472,** 90.

95 L. K. Nikam, R. Patil, R. Panmand , S. Kadam, K. Sivanandan and B. Kale , *Adv Sci Eng, Med.* 2013,**5 (7),** 688.